

Targeting Adeno-Associated Virus Vectors for Local Delivery to Fractures and Systemic Delivery to the Skeleton

Lucinda R. Lee,^{1,2} Lauren Peacock,¹ Leszek Lisowski,^{3,4} David G. Little,^{1,2} Craig F. Munns,^{2,5} and Aaron Schindeler^{1,2,3}

¹Orthopaedic Research and Biotechnology Unit, The Children's Hospital at Westmead, Westmead, NSW, Australia; ²The University of Sydney, Discipline of Child and Adolescent Health, Faculty of Health and Medicine, Sydney, NSW, Australia; ³Translational Vectorology Group, Children's Medical Research Institute, Faculty of Medicine and Health, The University of Sydney, Sydney, NSW 2006, Australia; ⁴Military Institute of Hygiene and Epidemiology, The Biological Threats Identification and Countermeasure Centre, 24-100 Pulawy, Poland; ⁵Institute of Endocrinology and Diabetes, The Children's Hospital at Westmead, Westmead, NSW, Australia

A panel of 18 recombinant adeno-associated virus (rAAV) variants, both natural and engineered, constitutively expressing Cre recombinase under the cytomegalovirus early enhancer/chicken β actin (CAG) promoter, were screened for their ability to transduce bone in Ai9 fluorescent reporter mice. Transgenic Cre-induced tdTomato expression served as a measure of transduction efficiency and alkaline phosphatase (AP) activity as an osteoblastic marker. Single injections of AAV8, AAV9, and AAV-DJ into midshaft tibial fractures yielded robust tdTomato expression in the callus. Next, the bone cell-specific promoters Sp7 and Col2.3 were tested to restrict Cre expression in an alternate model of systemic delivery by intravenous injection. Although CAG promoter constructs packaged into AAV8 produced high levels of tdTomato in the bone, liver, heart, spleen, and kidney, bone-specific promoter constructs restricted Cre expression to osseous tissues. AAV variants were further tested *in vitro* in a human osteoblast cell line (hFOB1.19), measuring GFP reporter expression by flow cytometry after 72 h. AAV2, AAV5, and AAV-DJ showed the highest transduction efficiency. In summary, we produced AAV vectors for selective and high-efficiency *in vivo* gene delivery to murine bone. The AAV8-Sp7-Cre vector has significant practical applications for inducing gene deletion postnatally in floxed mouse models.

INTRODUCTION

Viral vectors are effective delivery systems for safe and efficient delivery of therapeutic payloads to target cells *in vitro* and *in vivo*.¹ In particular, vectors derived from adeno-associated viruses (AAVs) have gained popularity in wide range of gene therapy applications because of their ease of manipulation, high transduction efficiency, and low immunogenic responses. Recombinant AAVs (rAAVs) have been shown to allow delivery of the components of the CRISPR/Cas9 system, the Cas9 endonuclease and RNA guides, to target cells and organs in pre-clinical models with high efficiency.² Although rAAVs have a relatively small packaging size (effective capacity of 4.4 kb), a 3.2-kb variant of Cas isolated from *Staphylococcus aureus* (saCas9) is small enough to be packaged into rAAV vectors.³

Gene editing in the context of the bone remains an underdeveloped field. Bone gene therapy has historically focused on local delivery of osteogenic proteins, such as bone morphogenetic proteins (BMPs).⁴ Recombinant AAV vectors targeted to fibroblasts or local osteoprogenitors to drive enhanced BMP expression have been used to induce local ectopic bone formation^{5–10} and promote fracture callus development^{11–13} and bone defect/osteotomy repair.^{14,15} However, in practical terms, such gene therapy technologies have relatively high associated risks compared with other regenerative medicine strategies, including exogenous scaffolds laden with cells and purified recombinant osteoinductive proteins. In contrast, there is a major clinical need to treat genetic bone fragility disorders such as osteogenesis imperfecta. Such gene therapy vectors would be required to have systemic efficacy rather than targeting focal bone defects. Furthermore, vectors relying on a BMP overexpression strategy may not adequately correct bone quality for patient mutations that affect collagen production or folding.

Nevertheless, gene targeting in a fracture healing scenario has a number of uses. For preclinical model development, it can be used to analyze the effects of gene overexpression or disruption on bone repair. This can be advantageous for genes where the associated mouse models have severe phenotypes that affect animal health or bone biomechanics. In this study, we used it as a screening modality to test a variety of AAV variants to identify those with a tropism for osteoblasts and osteocytes and/or skeletal tissues. A panel of 18 natural and engineered AAV variants was screened in a murine fracture model where vector-encoded Cre recombinase expression was detected via fluorescent tdTomato expression in the Ai9 reporter mouse strain (Figure 1).¹⁶ In addition to being a screening tool, identification of vectors that target fractures efficiently is a valuable tool for

Received 29 July 2019; accepted 26 August 2019;
<https://doi.org/10.1016/j.omtm.2019.08.010>.

Correspondence: Aaron Schindeler, PhD, Orthopaedic Research and Biotechnology Unit, Kids Research, The Children's Hospital at Westmead, Locked Bag 4001, Westmead, NSW 2145, Australia.

E-mail: aaron.schindeler@sydney.edu.au



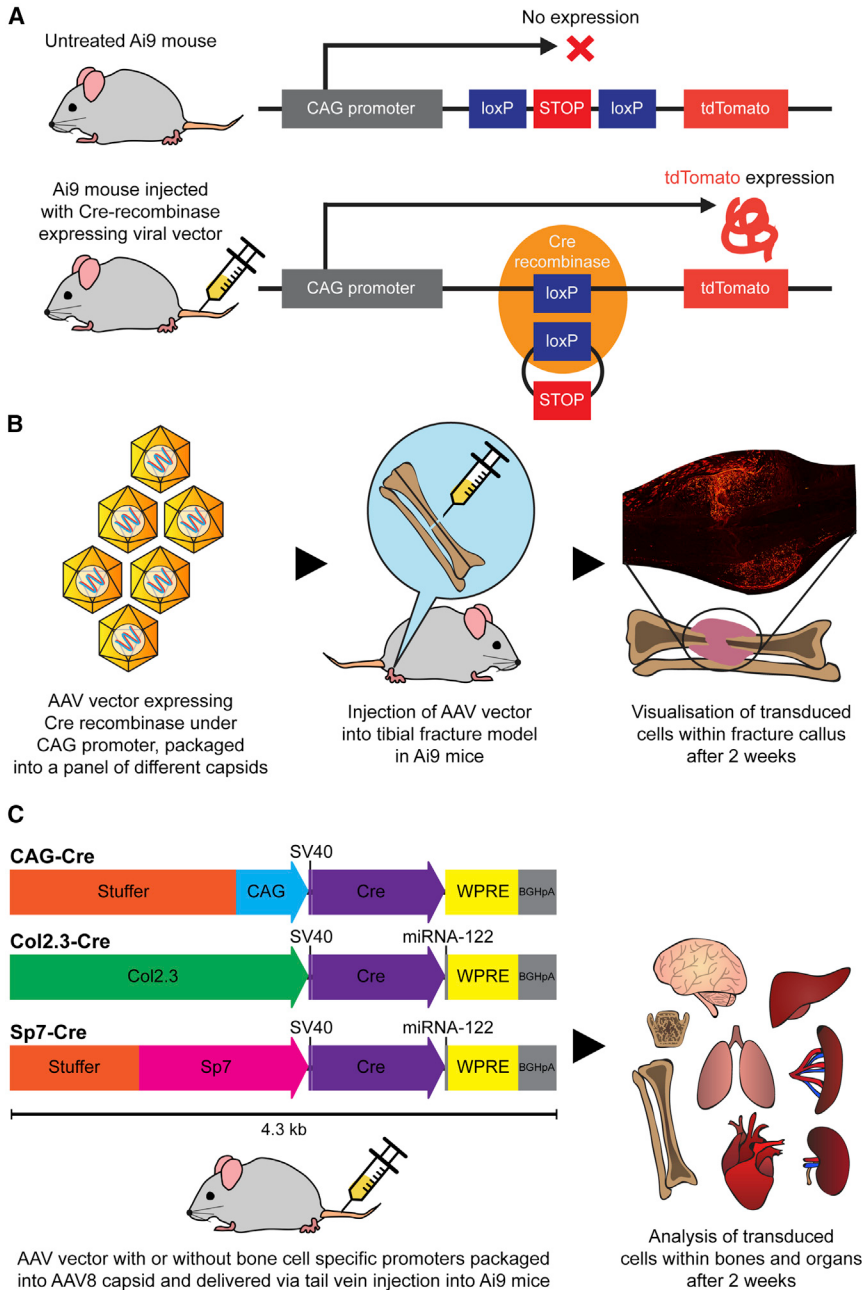


Figure 1. Ai9 Cre Reporter Mouse Strain and Study Plans for AAV Local and Systemic Delivery

(A) Ai9 Cre reporter mouse strain with tdTomato expression induced by Cre recombinase expressed by a viral vector, which excises the stop cassette upstream of the tdTomato expression cassette. (B) Study plan showing injection of the AAV vector containing Cre recombinase under the CAG constitutive promoter into a midshaft tibial fracture model in the Ai9 mouse. Analysis of tdTomato was performed 2 weeks post-transduction. (C) Study plan of systemic administration, showing AAV constructs expressing Cre recombinase under the CAG constitutive promoter and the bone cell-specific promoters Sp7 and Col2.3. Stuffer sequences were included on CAG and Sp7 constructs to match the size of the Col2.3 construct. Bovine growth hormone poly(A) (bGH_pA) and the woodchuck hepatitis virus (WHP) posttranscriptional regulatory element (WPRE) were included as enhancers. Analysis of tdTomato was performed 2 weeks post-transduction.

fragment^{19–22}) promoters, and functional transduction was detected using a Cre-activated fluorescent reporter in Ai9 transgenic mice (Figure 1). This represents the first comprehensive analysis of a large cohort of AAV variants for their ability to target bone and identifies several that achieve efficient and effective gene delivery to bone cells *in vivo*.

RESULTS

AAV8, AAV9, and AAV-DJ Efficiently Transduce the Fracture Callus

A healing fracture callus is a complex cellular microenvironment containing multiple cell types. Long-bone fractures also have adjacent musculature that can be unintentionally transduced by gene therapy vectors, leading to vector loss, increased cost of therapy, and decreased safety of potential gene therapy applications targeting bone fractures. We hypothesized that different variants of AAVs could have unique abilities to transduce bone cells within a healing fracture callus, and this was tested in a murine tibial fracture model following local injection.

All variants tested in our murine tibial fracture model showed some level of transduction of the skeletal muscle surrounding the fracture site (Table S1). The variants that showed high levels of tdTomato expression in skeletal muscle surrounding the callus were AAV1, AAV2, AAV3, AAV8, AAV9, AAV-DJ, AAV-DJ8, AAV-2i8, AAV-LK03, and AAV-Anc80.

Fifteen of the 18 variants tested gave a positive tdTomato signal within the callus; however, many were only able to transduce a small proportion of the cells in the callus; e.g., AAV3 and AAV-2i8

preclinical model development focused on the genetic determinants of fracture repair. This panel of AAV variants was screened in parallel in cultured human osteoblasts (hFOB1.19), where GFP transgene expression was measured by flow cytometry.

Next, AAV variants expressing Cre recombinase were trialed in mice using an intravenous (systemic) delivery approach. In this case, Cre recombinase was expressed either under a constitutively expressing cytomegalovirus early enhancer/chicken β actin (CAG) promoter (control group) or bone-specific (Sp7,^{17,18} Col1 2.3-kb

(Figure 2). Furthermore, AAV5, AAV6, AAV-LK02, and AAV-LK03 were able to transduce low numbers of callus cells but did not display a high level of co-localization with ELF 97 staining, indicating that they may have targeted cell types other than osteoblasts within the callus.

Importantly, the analysis showed that three vector variants, AAV8, AAV9, and AAV-DJ, were able to functionally transduce cells within the callus with high efficiency (Figure 2). Furthermore, AAV8 produced uniform fluorescence across the callus, whereas AAV-DJ showed high levels of transduction adjacent to the injection sites at either side of the callus. Representative images for each virus are shown because transduction efficiencies were consistent between samples.

Fluorescent alkaline phosphatase (AP) staining was performed using ELF 97 reagent and co-imaged with a tdTomato signal (Figure 3). Co-localization between AP and tdTomato expression was seen in specimens from animals administered AAV8, AAV9, and AAV-DJ, indicating that bone cells were transduced. A considerable number of tdTomato⁺/AP⁻ cells were within the callus surrounded by new bone. Based on location, morphology, and lack of AP expression, these were most likely new osteocytes.

AAV8 with Bone Cell-Specific Promoters Selectively Targets Osteoblasts following Systemic Administration

In a preliminary study, constructs driven by a ubiquitous CAG promoter packaged into AAV2, AAV8, and AAV-DJ were compared after intravenous injection of 5×10^{10} vector genome (vg)/mouse. Although some cells were targeted at this viral dose with AAV8, the relative numbers of tdTomato-positive cells within the bone compartment were low (Figure 4). Both AAV2 and AAV-DJ vectors showed negligible transduction in the tibiae. The AAV8-CAG-Cre construct was next compared with constructs driven by the bone cell-specific promoters Col2.3 and Sp7 following systemic administration. The use of bone cell-specific promoters restricted transgene expression mostly to bone cells (Figure 5); specifically, to cells positive for ELF 97 AP staining (namely, osteoblasts). Detailed analysis of the cells at higher magnification confirmed that the construct containing the CAG promoter led to transgene expression in cells other than osteoblasts (Figure 5), with larger cells on the bone surface consistent with osteoclasts and cells within the cortical bone consistent with osteocytes.

To increase the efficiency of transduction, the dose of AAV administered by single injection was increased 10-fold (5×10^{11} vg/mouse). This dramatically increased transduction of cells within the bone in the context of the AAV8 vector encoding the transgene under either of the three promoters (Figure 6) without any detectable adverse effects on animal health. Detailed analysis confirmed that transduction of osteoblasts within the growth plate and endochondral surface was greatly increased (Figure 6), and a high proportion of AP-negative osteocytes within the cortical bone was also affected with all constructs. Saliently, the Col2.3 and Sp7 constructs

showed negligible tdTomato expression outside of the bone, and at the bone surface, tdTomato co-expressed with the osteoblastic marker AP. It was also noted that Col2.3 showed transduction of periosteal and endosteal osteoblasts, whereas Sp7 showed mostly endosteal osteoblast transduction. High levels of tdTomato expression were also observed in the vertebrae (Figure S2). The CAG and Col2.3 promoters yielded robust tdTomato expression in the vertebrae, similar to the long bones. In contrast, reduced targeting of AP⁺ osteoblasts was observed in the vertebrae of the Sp7 group compared with the long bones of the same mice.

To examine the bone specificity of the three AAV constructs encoding individual promoters, tdTomato expression was analyzed in a range of tissues, including brain, heart, lung, liver, spleen, and kidney. The tissue expression profile of AAV8 harboring the CAG promoter was similar to that of a previously published AAV8-cytomegalovirus (CMV)-luciferase construct,²³ with robust expression in the heart and liver; low expression in the lung, spleen, and kidney; and undetectable expression in the brain. Cre recombinase activity in all tissues other than bone was greatly reduced in vectors encoding tissue-specific promoters (Col2.3 and Sp7) and posttranscriptional control (microRNA-122 target sequences) (Figure 7). Limited tdTomato signal was seen in the liver using the Col2.3 construct, although significantly less compared with the CAG construct. The Sp7 construct yielded minimal tdTomato expression in all non-skeletal tissues tested, with rare isolated tdTomato⁺ cells observed in the heart and liver.

Multiple AAV Variants Transduce Human Osteoblasts in Culture

The same panel of AAV variants was subsequently used to transduce a human fetal osteoblast (hFOB) cell line in culture. Seven of the 18 variants tested showed an ability to functionally transduce the cells and resulted in 14%–56% of GFP-positive cells (Figure 8). AAV2, AAV5, and AAV-DJ showed the highest levels. Unlike other osteoblastic cell lines, hFOB cells showed relatively high efficiency with plasmid lipofection, as evidenced by a control GFP plasmid (Figure 8). The variants effective for hFOBs showed high transduction rates at all MOIs tested. AAV-DJ was the only variant that showed high efficiency in the murine fracture model and in cultured human osteoblasts.

DISCUSSION

This paper describes a method for high-efficiency *in vivo* gene delivery to bone that is highly suitable for preclinical studies in mouse models of bone disease or injury. The AAV8 vector expressing Cre under the Sp7 promoter was able to systemically transduce osteoblasts at high efficiency, leading to a permanent recombination event marked by tdTomato expression. This vector has numerous applications in preclinical modeling of genetic disease and can be applied to conditional (*flaxed*) mouse models to create bone-specific knockout. The vector could also be applied locally to create knockout fractures, analogous to a previously published adenovirus model.²⁴ To date, there have been no studies demonstrating high-efficiency targeting of bone cells via a single systemic

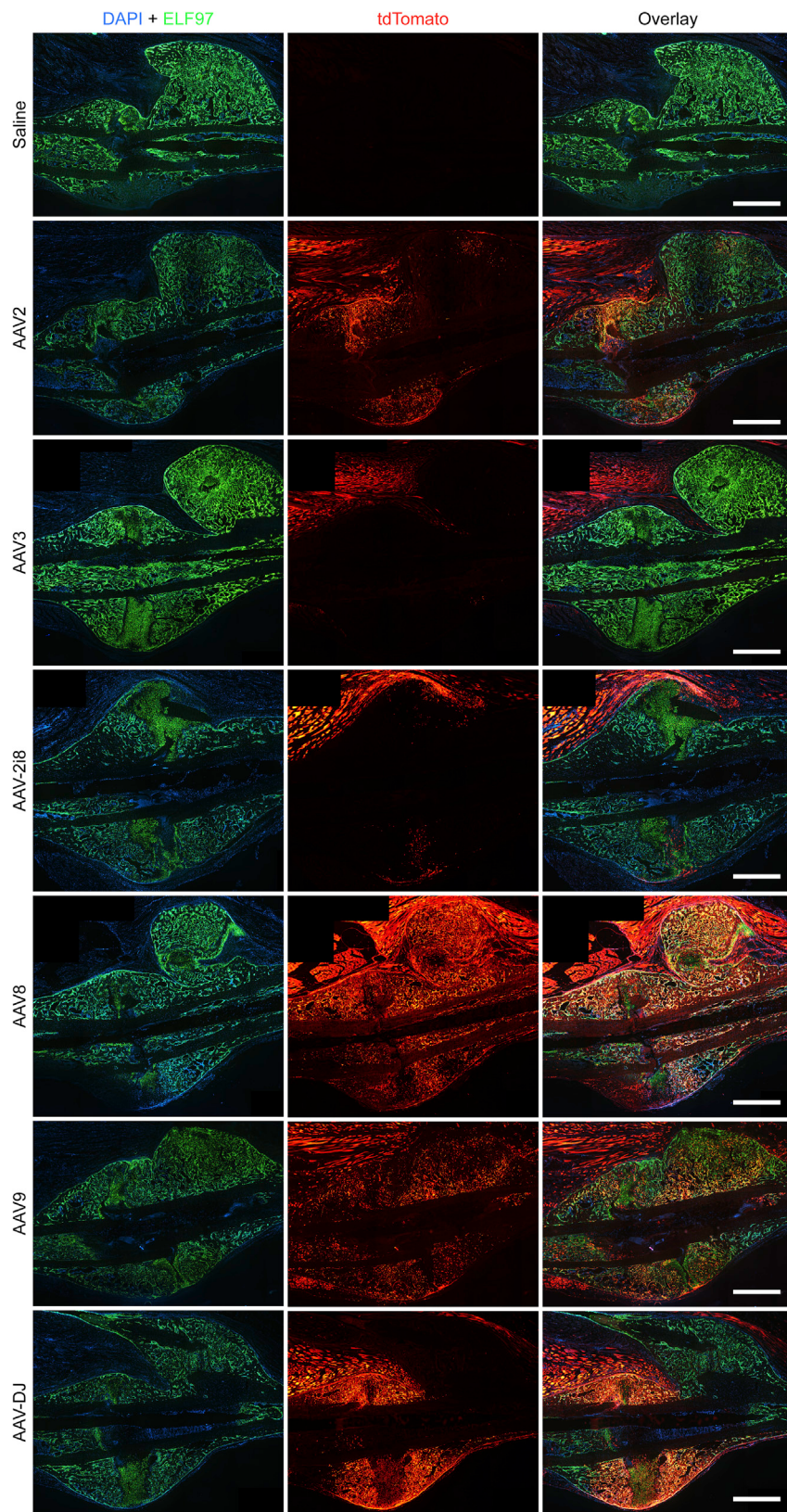


Figure 2. ELF 97 Fluorescent AP Substrate Staining of Representative Tibial Fracture Samples

AP-stained osteoblasts (green) were overlaid with the tdTomato signal for AAV transduction and Cre-mediated recombination (red). No tdTomato signal was seen in saline controls, and the majority of AAV vectors produced a negligible tdTomato signal in the fracture callus. AAV8-, AAV-DJ-, and AAV9-transduced specimens showed a considerable signal from both ELF 97 staining and tdTomato in the callus (yellow). Scale bars represent 1 mm.

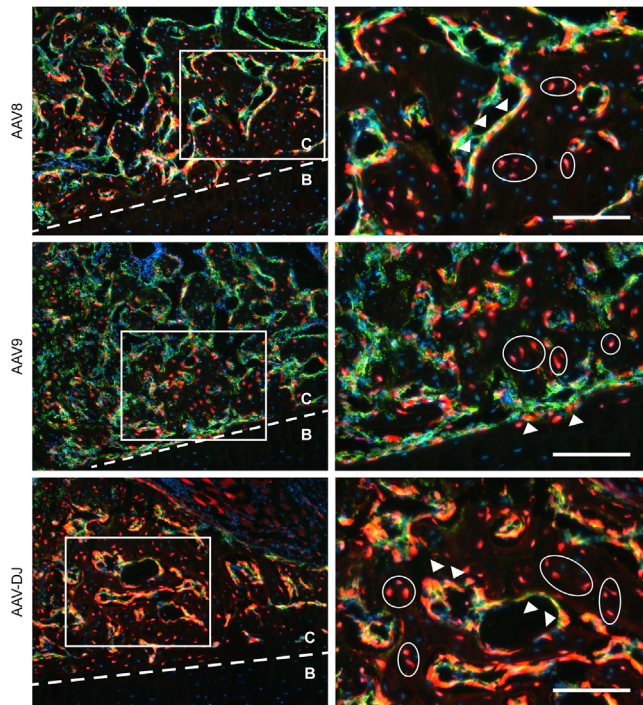


Figure 3. Higher-Power Images of ELF 97 Fluorescent AP Substrate Staining of Representative Tibial Fracture Samples

Images were collected from groups showing the highest transduction in the callus. Notably, negligible tdTomato expression was seen in osteocytes of the old cortical bone (B). ELF 97 labeled osteoblasts co-labeling with tdTomato (yellow) were present in the fracture callus (C; arrows). ELF-97-negative cells that were tdTomato+ putative osteocytes were present in the callus, surrounded by new bone matrix (C; circles). Scale bars represent 100 μ m.

dose of a viral vector; therefore, our findings represent a major technical advancement.

Two AAV variants, natural AAV8 and engineered AAV-DJ,²⁵ showed particularly utility for bone models. Both were able to transduce fracture calluses at high efficiency and may be useful for gene delivery or gene editing in fracture healing experiments. AAV8 was more effective in the systemic delivery model than AAV-DJ; however, AAV-DJ showed a higher efficiency in human osteoblasts. This is not unexpected because it has been shown that AAV-DJ is able to effectively transduce multiple human cell lines *in vitro*.²⁵ The poor efficiency of AAV-DJ following systemic delivery was comparable with that observed for AAV8 only at the lower vector dose, and it could be hypothesized that AAV-DJ may show levels of bone transduction at higher doses. Nevertheless, the comparative superiority of AAV8 made it the capsid of choice for future studies.

AAV8 is a natural AAV variant isolated from rhesus monkey tissues, and it has been shown to have high efficiency in liver transduction in mice, reported to be 10–100 times higher than that of AAV2.^{26,27} The most significant structural differences between AAV8 and AAV2 are

situated on the surface of the capsid in areas reported to be involved in interactions with cellular receptors and anti-AAV2 antibody binding sites.²⁷ Approximately 60%–80% of the human population harbors antibodies to AAV2, and because AAV8 shows increased resistance to these antibodies and has a higher liver transduction, it has been used successfully in clinical trials for the treatment of hemophilia B.²⁸ Notably, despite AAV8's high efficiency at transduction of mouse liver, in our studies, use of the Sp7 promoter and microRNA-122^{29,30} prevented transgene expression in the liver. Although some sporadic tdTomato+ cells were seen in other organs, the overall numbers were low and could potentially be attributed to transduced mesenchymal stem cells (MSCs) because these cells, which are primarily found in the bone marrow niche and are osteoblast precursors, have been shown to reside in many tissues in close proximity to blood vessels.^{31,32}

AAV-DJ is an engineered variant composed of elements from AAV2, AAV8, and AAV9, which was selected for its ability to transduce cells in the presence of human neutralizing monoclonal antibodies,³³ making it useful for human translation. Our finding of AAV-DJ being able to produce high-efficiency transduction of bone cells within a callus is consistent with the findings of another group that used AAV-DJ to deliver a COX2 transgene locally in a murine fracture model to promote bone healing.¹¹ Comparing AAV-DJ with AAV2 for transgene delivery, the authors found AAV-DJ to support faster kinetics and significantly higher transgene expression in the fracture site, and *in vitro*, AAV-DJ produced an approximately 5-fold increase in transduction of murine MSCs. However, their conclusion that this vector would be applicable to humans was not tested. We have shown that AAV-DJ was able to effectively transduce a human osteoblast cell line *in vitro*. However, because cell lines are not always biologically predictive and may not predict function *in vivo*, further testing in other models, such as non-human primates, will be needed to evaluate AAV-DJ's clinical applicability and translational potential. Nevertheless, these data are presented in the context of a broader panel of variants screened, which identified a range of AAVs with human bone potential. This is important because the tropism of AAV capsids does not always correlate between species.

AAVs have been used to deliver CRISPR/Cas9 constructs *in vivo* to successfully mediate gene editing in muscle² but not yet in the context of bone. Despite the size constraints of AAV constructs, splitting the Cas9 protein sequence between two AAVs and using N- and C-terminal intein sequences to fuse both peptides after translation has proven to be highly effective for CRISPR *in vivo*.³⁴ CRISPR/Cas9 gene editing under control of the Sp7 promoter using AAV8 constructs is a goal of our future studies. The Ai9 mouse line used in this study is also a convenient model for testing CRISPR gene editing, making use of validated guides that target the stop cassette upstream of the tdTomato locus.²

Engineered AAV variants have great potential for use in bone, specifically in genetic bone conditions. There is potential for AAV

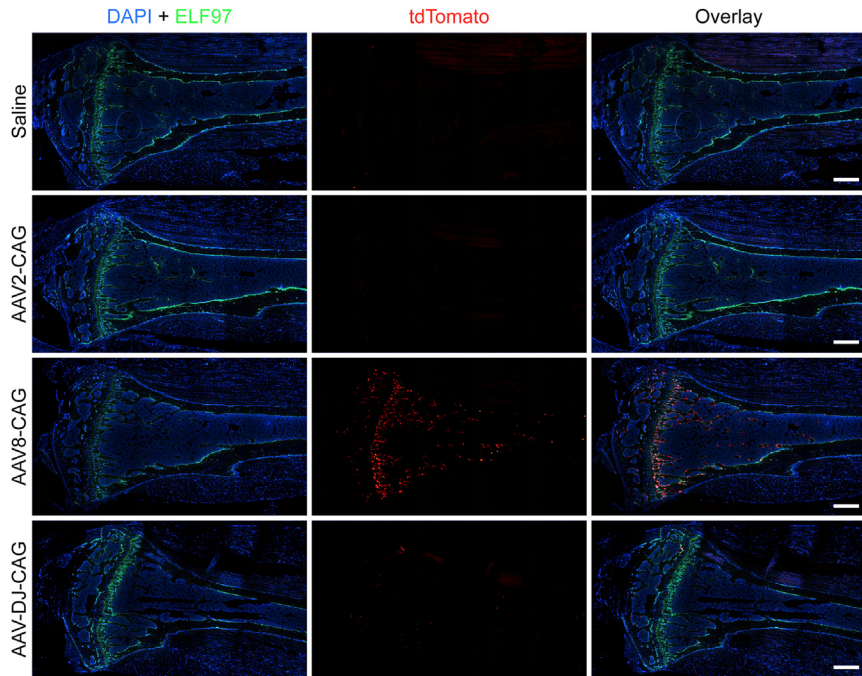


Figure 4. ELF 97 Fluorescent AP Substrate Staining of Representative Tibial Samples

AP-stained osteoblasts (green) were overlaid with the tdTomato signal for AAV transduction and Cre-mediated recombination (red). Constructs packaged in the AAV8 capsid showed the highest tdTomato expression and, hence, transduction rate in tibial samples. Scale bars represent 500 μ m.

able to drive high transgene expression in mammalian expression vectors.^{40,41}

Both CAG and Sp7 constructs included non-functional “stuffer” sequences to maintain constant construct length because construct size can effect transduction efficiency.⁴² The woodchuck hepatitis virus posttranscriptional regulatory element (WPRE) was also included as an enhancer because it introduces a tertiary structure that is capable of enhancing the expression of transgenes carried by viral vectors.⁴³ Bovine growth hormone poly(A) (bGHpA) was used as a terminator sequence

in the constructs because it has been shown to be more effective than synthetic poly(A) tails.⁴³ All constructs were designed *in silico* to contain all required regulatory elements and stuffer sequences to ensure identical total size between constructs. Following *in silico* design, all constructs were custom synthesized (Genewiz, South Plainfield, NJ, USA).

All rAAV stocks were prepared by polyethylenimine (PEI) (Polysciences, Warrington, PA, USA) triple transfection (2:1 PEI:DNA ratio) of adherent HEK293T cells (CRL-3126; ATCC, Manassas, VA, USA) with a pAd5 helper plasmid,⁴⁴ AAV transfer vector, and AAV-helper plasmid encoding *rep2* and the capsid of interest at 2:1:1 molar ratios. Cell lysates from five 15-cm dishes were pooled and purified using iodixanol-based density gradients as described previously.⁴⁵ Amicon Ultra-4 centrifuge filter units with Ultracel-100-kDa membranes (EMD Millipore, Burlington, MA, USA) were used to perform a buffer exchange (PBS, 50 mM NaCl, 0.001% Pluronic F68 [v/v]; Thermo Fisher Scientific, Waltham, MA, USA) and a concentration step.

Mouse Strains and Husbandry

Ai9 mice (The Jackson Laboratory [JAX] stock number 007909), a Cre reporter mouse strain with a tdTomato red fluorescent reporter gene,¹⁶ were bred to heterozygosity with C57BL/6J (wild-type [WT]) mice sourced from the Animal Resources Centre (Perth, Australia). All experimental mice were heterozygote females group housed and given food and water *ad libitum*.

Mice for fracture experiments were aged 10 weeks at the time of surgery. Mice for systemic injection experiments were aged 8 weeks

vectors to be used in functional genomics studies to induce disease-causing mutations and model genetic bone conditions. Ultimately however, this technology may be capable of correcting pathogenic mutations in patients. Historically, gene therapy targeting bone has focused on intramuscular delivery, introducing factors skeletal muscle cells produce to stimulate bone cells located in close proximity.³⁵ However, with the generation of engineered AAV variants enabling direct targeting of bone cells, including osteoblasts, osteocytes, osteoclasts and their precursors, (pre)clinical applications requiring both local and systemic delivery became achievable.

MATERIALS AND METHODS

Virus Production

18 different AAV variants were tested for their efficiency of transducing cells *in vivo* within a tibial fracture callus and *in vitro* in human and murine osteoblastic cell lines. The variants tested all contained the same construct, CAG-Cre-GFP, packaged into different AAV capsids (Table S1). Natural variants tested were AAV1, AAV2, AAV3, AAV4, AAV5, AAV6, AAV8, AAV9, and AAVrh10.³⁶ Engineered variants tested were AAV-2i8;³⁷ AAV-7m8;³⁸ AAV-DJ and AAV-DJ8;²⁵ AAV-LK01, AAV-LK02, AAV-LK03, and AAV-LK19;²⁶ and AAV-Anc80.³⁹

For systemic delivery, three different constructs were packaged into AAV8 capsids (Figure 1C). Constructs containing Cre recombinase were driven by the ubiquitous promoter CAG or the bone cell-specific promoters Col2.3 or Sp7. CAG is a synthetic promoter consisting of the CMV early enhancer element, the promoter and first and second introns of the chicken β -actin gene, and the splice acceptor of the rabbit β -globin gene.^{40,41} It is a strong promoter

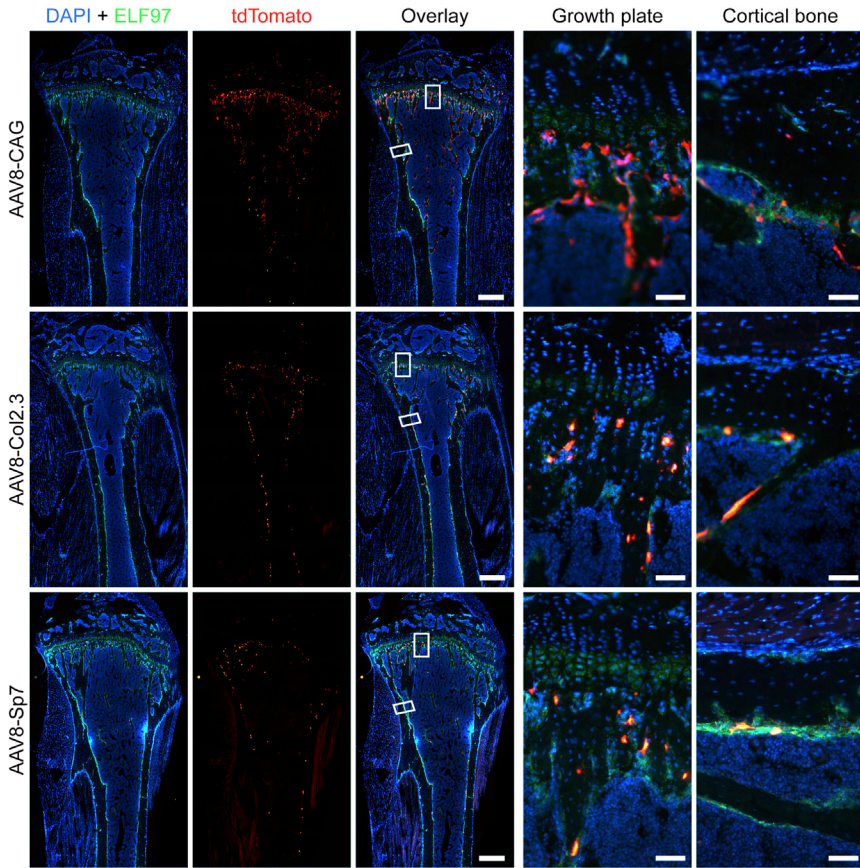


Figure 5. ELF 97 Fluorescent AP Substrate Staining of Representative Tibial Samples

AP-stained osteoblasts (green) were overlaid with the tdTomato signal for AAV transduction and Cre-mediated recombination (red). All constructs showed levels of transduction in tibiae. The CAG ubiquitous promoter showed a higher level; however, the bone-specific promoters Col2.3 and Sp7 showed, relatively, the same level of transduction that co-localized with ELF 97 labeled osteoblasts. Scale bars represent 500 μ m; scale bars on cortical bone and growth plate images represent 50 μ m.

at the time of injection. Animal experiments were approved by The Children's Hospital at Westmead/Children's Medical Research Institute Animal Ethics Committee under protocols K350 and K357.

Mouse Fracture AAV Delivery Study Design

A panel of 18 variants of AAV (Table S1) was tested in Ai9 mice ($n = 3$ mice per group). A saline only group was included as a negative control ($n = 3$). Animals were sacrificed 14 days after vector delivery to examine transduced cells that had undergone genetic recombination to express tdTomato.

Fracture Surgery and AAV Delivery

Female mice aged 10 weeks were used in closed fracture experiments. In preparation for surgery, mice were anesthetized with ketamine (35 mg/kg) and xylazine (4.5 mg/kg) intraperitoneally and maintained using inhaled isoflurane. Tibial midshaft fractures were generated by experienced staff. Through a small incision below the knee made with a 27G needle, an intramedullary rod (0.3-mm-diameter stainless steel insect pin) was surgically inserted into the medullary canal of the tibia. A modified set of surgical staple removers was used to generate fractures manually by three-point bending. Fractures were confirmed via X-ray (Faxitron X-ray, Tuc-

son, AZ, USA) to be transverse, above the fibular junction, and without comminution.

10 μ L of viral stock solution was diluted with 50 μ L isotonic sterile saline and injected into the fracture site bilaterally, with half of the solution injected into the soft tissue on each side of the tibia. A 29G insulin needle with a 1-mL syringe (Terumo, Shibuya, Japan) was used for each injection, with the needle inserted until it touched the tibia and then pulled slightly away from the bone surface for injection. Post-surgical pain was managed using buprenorphine (0.05 mg/kg subcutaneously, every 12 h as required). Fracture repair and pin stability were monitored weekly by X-ray. At the experimental endpoint of 14 days, animals were euthanized with carbon dioxide, and specimens were collected post-mortem for histology.

Systemic AAV Administration Study Design

AAV-8 containing constructs driven by the CAG, Col2.3, and Sp7 promoters were tested in Ai9 mice ($n = 4$ mice per group), with a saline-only group included as a negative control ($n = 4$). Animals were sacrificed 14 days after vector delivery to examine transduced cells that had undergone genetic recombination to express tdTomato in bones and other tissues.

Systemic Injection AAV Delivery

Viral stocks were diluted in 200 μ L isotonic sterile saline to doses of 5×10^{10} vg/mouse for the initial trial and 5×10^{11} vg/mouse for the higher-dose follow-up. Mice were temporarily anesthetized using inhaled isoflurane and restrained while the viral solution was injected into the tail vein using a 27G needle. Mice were closely monitored for 3 days after injection, then weekly. At the experimental endpoint of 14 days, animals were euthanized with carbon dioxide, and specimens were collected post-mortem for histology.

Histological Analysis

Fractured and non-fractured tibiae were removed with surrounding soft tissue intact, along with femora and L3 vertebrae. The

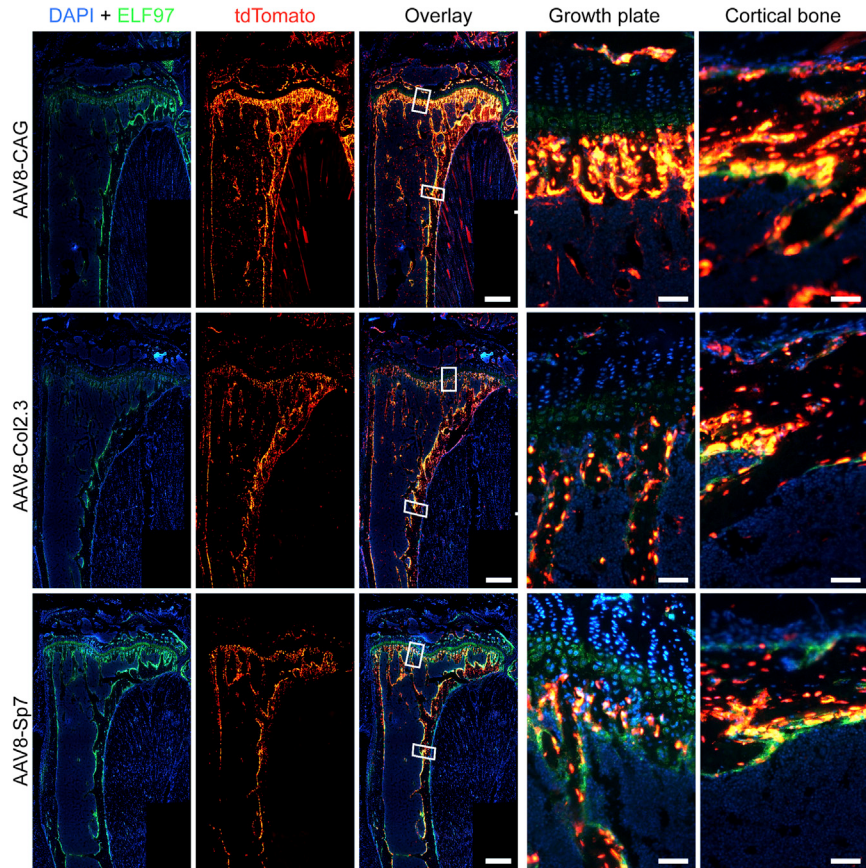


Figure 6. ELF 97 Fluorescent AP Substrate Staining of Representative Tibial Samples from Mice Receiving 5×10^{11} vg of AAV Constructs

AP-stained osteoblasts (green) were overlaid with the tdTomato signal for AAV transduction and Cre-mediated recombination (red). All constructs showed a higher level of transduction in tibiae with the increased viral dose. The bone-specific promoters Col2.3 and Sp7 showed similar levels of transduction that co-localized with ELF-97-labeled osteoblasts. Notably, an increased number of transduced osteocytes within cortical bone was achieved with the increased AAV dose. Scale bars on whole-tibia images represent 500 μ m; scale bars on cortical bone and growth plate images represent 50 μ m.

Scientific, Waltham, MA, USA) for nuclear staining, mounted with CC Mount (Sigma-Aldrich, St. Louis, MO, USA), and coverslipped for imaging.

Microscopic Imaging

ELF 97- and DAPI-stained sections were observed with a DMi8 inverted wide-field fluorescence microscope (Leica Microsystems, Wetzlar, Germany) with a 10 \times objective. A DAPI longpass filter was used to concurrently illuminate DAPI and ELF 97, and the color camera was used to capture both signals. A Texas red filter was used to illuminate tdTomato. Tile scan images in both channels of entire tibial fracture calluses, proximal tibial

epiphyses, L3 vertebrae, and organs were taken and stitched upon capture in LASX software (Leica Microsystems, Wetzlar, Germany).

Cell Culture

The 18 AAV variants were tested *in vitro* using hFOB1.19 cells (CRL-11372, ATCC, Manassas, VA, USA), an immortalized hFOB cell line.⁴⁶ Cells were seeded into well plates with DMEM/F12 medium (Thermo Fisher Scientific, Waltham, MA, USA) supplemented with 10% FBS and penicillin/streptomycin (Thermo Fisher Scientific, Waltham, MA, USA) to achieve a confluence of 70% at transduction. The viral suspension was added to each well, using four different MOIs for each vector, with the MOIs ranging from 1×10^4 to 5×10^5 vg/cell (Figure S1). After 72 h, cells were washed with PBS, detached from the plate with trypsin (Thermo Fisher Scientific, Waltham, MA, USA), and fixed in 10% neutral buffered formalin (Thermo Fisher Scientific, Waltham, MA) for 10 min. Cells were washed and resuspended in fluorescence-activated cell sorting (FACS) buffer (PBS [Thermo Fisher Scientific, Waltham, MA, USA], 1% FBS [Thermo Fisher Scientific, Waltham, MA, USA], and 0.01M EDTA [Astral Scientific, Taren Point, Australia]) in FACS tubes for analysis (BD Biosciences, Franklin Lakes, NJ, USA).

brain, heart, lungs, spleen, liver, and kidneys were also removed. All tissues were fixed overnight in 10% neutral buffered formalin at 4°C. Care was taken to protect samples from light throughout histological processing because of the tdTomato fluorescence present in the samples. Samples were then changed to 30% sucrose for a further 12 h at 4°C. All samples were cryo-embedded in Tissue-Tek OCT Compound (Sakura Finetek USA, Torrance, CA, USA) using an isopentane bath suspended in liquid nitrogen and stored at -80°C until cryosectioning.

Tibiae were sectioned on a cryostat at 5 μ m using the tape transfer method on cryotape (Section-lab, Hiroshima, Japan). Tape sections were adhered to uncoated glass microscope slides using chitosan solution (1% chitosan [Sigma-Aldrich, St. Louis, MO, USA] in 0.25% acetic acid [Sigma-Aldrich, St. Louis, MO, USA]) and left to dry at 4°C.

Tibial sections were stained with the ELF 97 Endogenous Phosphatase Detection Kit (Thermo Fisher Scientific, Waltham, MA, USA), a substrate that forms a strong yellow/green fluorescent precipitate in the presence of AP. The standard staining protocol for the reagent was followed to detect AP activity and, hence, labeled osteoblasts. These sections were co-stained with DAPI (Thermo Fisher

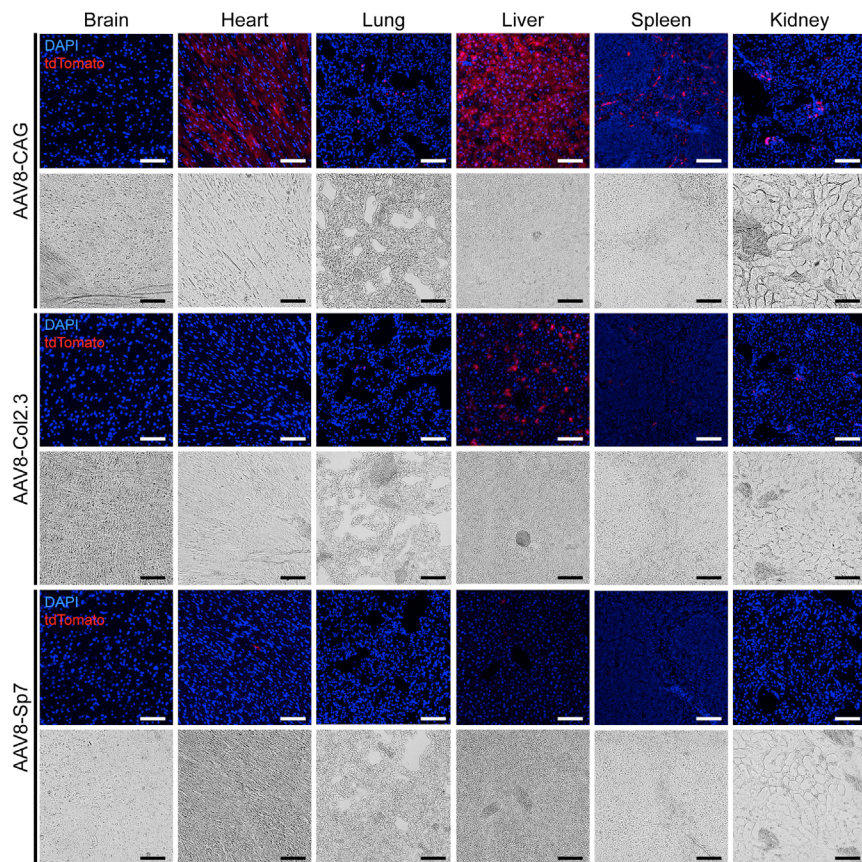


Figure 7. Representative Cryosections of Brain, Heart, Lung, Liver, Spleen, and Kidney from Ai9 Mice Receiving 5×10^{11} vg of AAV Constructs

Fluorescent overlays and corresponding bright-field images are shown. The CAG constitutive promoter construct is highly expressed in the heart and liver and, to a lesser extent, expressed in the lung, spleen and kidney. The Col2.3 and Sp7 constructs include bone cell-specific promoters and microRNA-122 sequences in an effort to mitigate off-target expression. Liver expression of Cre recombinase is significantly reduced in these groups, with almost no expression with Sp7. Expression of Cre recombinase is reduced in all tissues examined from the bone cell-specific promoter groups. Scale bars represent 100 μ m.

Flow Cytometry/FACS

Cells were analyzed for GFP fluorescence using FACSCanto (BD Biosciences, Franklin Lakes, NJ, USA) with a blue laser (emission, 502 nm). Flow data were analyzed using FACSDiva software (BD Biosciences, Franklin Lakes, NJ, USA). The percentage of GFP+ cells was determined based on gating for the non-transduced cells, and cells were transfected with GFP plasmid using

Lipofectamine 3000 (Thermo Fisher Scientific, Waltham, MA, USA). This was done because it is known that transfected cells will emit some GFP fluorescence, and virally transduced cells usually display a higher amount of fluorescence at high MOIs; hence, the upper threshold was set past this sample to capture brighter cells. A true positive control was not able to be used because there is no evidence in the literature to suggest that

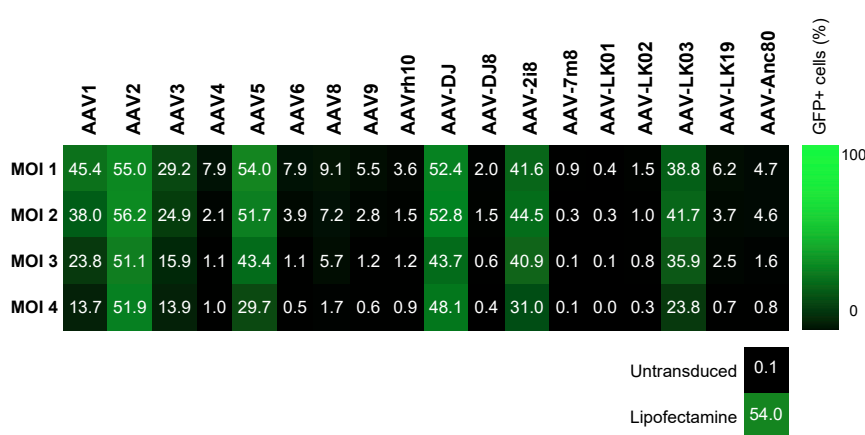


Figure 8. Percentage of GFP+ hFOB1.19 Cells Detected by Flow Cytometry after Transduction with the AAV Panel

Osteoblast cells were transduced at four different MOIs that were adjusted based on stock titers. MOIs ranged from 1×10^4 to 5×10^5 vg/cell, with the highest MOI tested for each AAV indicated by MOI 1 and the lowest by MOI 4 (vg per cell are given for each MOI in Table S1).

the hFOB cell line has been transduced previously using AAV vectors.

SUPPLEMENTAL INFORMATION

Supplemental Information can be found online at <https://doi.org/10.1016/j.omtm.2019.08.010>.

AUTHOR CONTRIBUTIONS

L.R.L. performed the bulk of the experiments and data analyses. L.P. performed animal surgery and animal care. L.L. provided the panel of AAV variants and designed, cloned, and packaged custom AAV constructs. D.G.L., C.F.M., and A.S. conceived the study, designed the experimental plan, and assisted with data analysis and interpretation of results. L.R.L. and A.S. drafted the manuscript, with all authors providing critical feedback and revisions.

ACKNOWLEDGMENTS

This work was supported by funding from the Care 4 Brittle Bones Foundation, the Sticks and Stones Foundation of Australia, and the Paediatric organization. L.R.L. was supported by an Australian Government Research Training Program (RTP) scholarship. L.L. was supported by a project grant from the Australian National Health and Medical Research Council (NHMRC; APP1108311). The authors wish to thank Dr Laurence Cantrill for assistance with the DMi8 microscope.

REFERENCES

- Ginn, S.L., Amaya, A.K., Alexander, I.E., Edelstein, M., and Abedi, M.R. (2018). Gene therapy clinical trials worldwide to 2017: An update. *J. Gene Med.* **20**, e3015.
- Tabebordbar, M., Zhu, K., Cheng, J.K.W., Chew, W.L., Widrick, J.J., Yan, W.X., Maesner, C., Wu, E.Y., Xiao, R., Ran, F.A., et al. (2016). In vivo gene editing in dystrophic mouse muscle and muscle stem cells. *Science* **351**, 407–411.
- Ran, F.A., Cong, L., Yan, W.X., Scott, D.A., Gootenberg, J.S., Kriz, A.J., Zetsche, B., Shalem, O., Wu, X., Makarova, K.S., et al. (2015). In vivo genome editing using *Staphylococcus aureus* Cas9. *Nature* **520**, 186–191.
- Virk, M.S., Conduah, A., Park, S.-H., Liu, N., Sugiyama, O., Cuomo, A., Kang, C., and Lieberman, J.R. (2008). Influence of short-term adenoviral vector and prolonged lentiviral vector mediated bone morphogenetic protein-2 expression on the quality of bone repair in a rat femoral defect model. *Bone* **42**, 921–931.
- Lieberman, J.R., Le, L.Q., Wu, L., Finerman, G.A., Berk, A., Witte, O.N., and Stevenson, S. (1998). Regional gene therapy with a BMP-2-producing murine stromal cell line induces heterotopic and orthotopic bone formation in rodents. *J. Orthop. Res.* **16**, 330–339.
- Musgrave, D.S., Bosch, P., Ghivizzani, S., Robbins, P.D., Evans, C.H., and Huard, J. (1999). Adenovirus-mediated direct gene therapy with bone morphogenetic protein-2 produces bone. *Bone* **24**, 541–547.
- Chen, Y., Cheung, K.M., Kung, H.F., Leong, J.C., Lu, W.W., and Luk, K.D. (2002). In vivo new bone formation by direct transfer of adenoviral-mediated bone morphogenetic protein-4 gene. *Biochem. Biophys. Res. Commun.* **298**, 121–127.
- Chen, Y., Luk, K.D., Cheung, K.M., Xu, R., Lin, M.C., Lu, W.W., Leong, J.C., and Kung, H.F. (2003). Gene therapy for new bone formation using adeno-associated viral bone morphogenetic protein-2 vectors. *Gene Ther.* **10**, 1345–1353.
- Luk, K.D., Chen, Y., Cheung, K.M., Kung, H.F., Lu, W.W., and Leong, J.C. (2003). Adeno-associated virus-mediated bone morphogenetic protein-4 gene therapy for in vivo bone formation. *Biochem. Biophys. Res. Commun.* **308**, 636–645.
- Chen, Y., Luk, K.D., Cheung, K.M., Lu, W.W., An, X.M., Ng, S.S., Lin, M.C., and Kung, H.F. (2004). Combination of adeno-associated virus and adenovirus vectors expressing bone morphogenetic protein-2 produces enhanced osteogenic activity in immunocompetent rats. *Biochem. Biophys. Res. Commun.* **317**, 675–681.
- Lakhan, R., Baylink, D.J., Lau, K.H., Tang, X., Sheng, M.H., Rundle, C.H., and Qin, X. (2015). Local administration of AAV-DJ pseudoserotype expressing COX2 provided early onset of transgene expression and promoted bone fracture healing in mice. *Gene Ther.* **22**, 721–728.
- Zachos, T., Diggs, A., Weisbrode, S., Bartlett, J., and Bertone, A. (2007). Mesenchymal stem cell-mediated gene delivery of bone morphogenetic protein-2 in an articular fracture model. *Mol. Ther.* **15**, 1543–1550.
- Ulrich-Vinther, M., Schwarz, E.M., Pedersen, F.S., Søballe, K., and Andreassen, T.T. (2005). Gene therapy with human osteoprotegerin decreases callus remodeling with limited effects on biomechanical properties. *Bone* **37**, 751–758.
- Müller, C.W., Hildebrandt, K., Gerich, T., Krettek, C., Griensven, M., and Rosado Balmayor, E. (2015). BMP-2-transduced human bone marrow stem cells enhance neo-bone formation in a rat critical-sized femur defect. *J. Tissue Eng. Regen. Med.* **11**, 1122–1131.
- Yazici, C., Takahata, M., Reynolds, D.G., Xie, C., Samulski, R.J., Samulski, J., Beecham, E.J., Gertzman, A.A., Spilker, M., Zhang, X., et al. (2011). Self-complementary AAV2.5-BMP2-coated femoral allografts mediated superior bone healing versus live autografts in mice with equivalent biomechanics to unfractured femur. *Mol. Ther.* **19**, 1416–1425.
- Madisen, L., Zwingman, T.A., Sunkin, S.M., Oh, S.W., Zariwala, H.A., Gu, H., Ng, L.L., Palmiter, R.D., Hawrylycz, M.J., Jones, A.R., et al. (2010). A robust and high-throughput Cre reporting and characterization system for the whole mouse brain. *Nat. Neurosci.* **13**, 133–140.
- Lu, X., Gilbert, L., He, X., Rubin, J., and Nanes, M.S. (2006). Transcriptional regulation of the osterix (Osx, Sp7) promoter by tumor necrosis factor identifies disparate effects of mitogen-activated protein kinase and NF κ B pathways. *J. Biol. Chem.* **281**, 6297–6306.
- Zhang, C., Cho, K., Huang, Y., Lyons, J.P., Zhou, X., Sinha, K., McCrea, P.D., and de Crombrugghe, B. (2008). Inhibition of Wnt signaling by the osteoblast-specific transcription factor Osterix. *Proc. Natl. Acad. Sci. USA* **105**, 6936–6941.
- Marijanović, I., Jiang, X., Kronenberg, M.S., Stover, M.L., Erceg, I., Lichtler, A.C., and Rowe, D.W. (2003). Dual reporter transgene driven by 2.3Col1a1 promoter is active in differentiated osteoblasts. *Croat. Med. J.* **44**, 412–417.
- Dacquin, R., Starbuck, M., Schinke, T., and Karsenty, G. (2002). Mouse α 1(I)-collagen promoter is the best known promoter to drive efficient Cre recombinase expression in osteoblast. *Dev. Dyn.* **224**, 245–251.
- Rosser, J., Eberspaecher, H., and de Crombrugghe, B. (1995). Separate cis-acting DNA elements of the mouse pro-alpha 1(I) collagen promoter direct expression of reporter genes to different type I collagen-producing cells in transgenic mice. *J. Cell Biol.* **129**, 1421–1432.
- Liu, F., Woitge, H.W., Braut, A., Kronenberg, M.S., Lichtler, A.C., Mina, M., and Kream, B.E. (2004). Expression and activity of osteoblast-targeted Cre recombinase transgenes in murine skeletal tissues. *Int. J. Dev. Biol.* **48**, 645–653.
- Zincarelli, C., Solty, S., Rengo, G., and Rabinowitz, J.E. (2008). Analysis of AAV serotypes 1–9 mediated gene expression and tropism in mice after systemic injection. *Mol. Ther.* **16**, 1073–1080.
- El-Hoss, J., Sullivan, K., Cheng, T., Yu, N.Y., Bobyn, J.D., Peacock, L., Mikulec, K., Baldoock, P., Alexander, I.E., Schindeler, A., and Little, D.G. (2012). A murine model of neurofibromatosis type 1 tibial pseudarthrosis featuring proliferative fibrous tissue and osteoclast-like cells. *J. Bone Miner. Res.* **27**, 68–78.
- Grimm, D., Lee, J.S., Wang, L., Desai, T., Akache, B., Storm, T.A., and Kay, M.A. (2008). In vitro and in vivo gene therapy vector evolution via multispecies interbreeding and retargeting of adeno-associated viruses. *J. Virol.* **82**, 5887–5911.
- Lisowski, L., Dane, A.P., Chu, K., Zhang, Y., Cunningham, S.C., Wilson, E.M., Nygaard, S., Grompe, M., Alexander, I.E., and Kay, M.A. (2014). Selection and evaluation of clinically relevant AAV variants in a xenograft liver model. *Nature* **506**, 382–386.
- Nam, H.-J., Lane, M.D., Padron, E., Gurda, B., McKenna, R., Kohlbrenner, E., Aslanidi, G., Byrne, B., Muzyczka, N., Zolotukhin, S., and Agbandje-McKenna, M. (2007). Structure of adeno-associated virus serotype 8, a gene therapy vector. *J. Virol.* **81**, 12260–12271.

28. Wang, L., Wilson, J.M., Calcedo, R., Bell, P., He, Z., White, J., et al. (2016). Strategies for Selection of AAV Vectors for Administration to Liver: Studies in Nonhuman Primates. *Blood* 128, 2316.
29. Brown, B.D., Gentner, B., Cantore, A., Colleoni, S., Amendola, M., Zingale, A., Baccarini, A., Lazzari, G., Galli, C., and Naldini, L. (2007). Endogenous microRNA can be broadly exploited to regulate transgene expression according to tissue, lineage and differentiation state. *Nat. Biotechnol.* 25, 1457–1467.
30. Qiao, C., Yuan, Z., Li, J., He, B., Zheng, H., Mayer, C., Li, J., and Xiao, X. (2011). Liver-specific microRNA-122 target sequences incorporated in AAV vectors efficiently inhibits transgene expression in the liver. *Gene Ther.* 18, 403–410.
31. Breitbach, M., Kimura, K., Luis, T.C., Fuegmann, C.J., Woll, P.S., Hesse, M., Facchini, R., Rieck, S., Jobin, K., Reinhardt, J., et al. (2018). In Vivo Labeling by CD73 Marks Multipotent Stromal Cells and Highlights Endothelial Heterogeneity in the Bone Marrow Niche. *Cell Stem Cell* 22, 262–276.e7.
32. da Silva Meirelles, L., Chagastelles, P.C., and Nardi, N.B. (2006). Mesenchymal stem cells reside in virtually all post-natal organs and tissues. *J. Cell Sci.* 119, 2204–2213.
33. Lerch, T.F., O'Donnell, J.K., Meyer, N.L., Xie, Q., Taylor, K.A., Stagg, S.M., and Chapman, M.S. (2012). Structure of AAV-DJ, a retargeted gene therapy vector: cryo-electron microscopy at 4.5 Å resolution. *Structure* 20, 1310–1320.
34. Moreno, A.M., Fu, X., Zhu, J., Katrekar, D., Shih, Y.-R.V., Marlett, J., et al. (2018). In Situ Gene Therapy via AAV-CRISPR-Cas9-Mediated Targeted Gene Regulation. *Mol. Ther.* 26, 181–1827.
35. Bulaklak, K., and Xiao, X. (2017). Therapeutic advances in musculoskeletal AAV targeting approaches. *Curr. Opin. Pharmacol.* 34, 56–63.
36. Gao, G., Vandenberghe, L.H., Alvira, M.R., Lu, Y., Calcedo, R., Zhou, X., and Wilson, J.M. (2004). Clades of Adeno-associated viruses are widely disseminated in human tissues. *J. Virol.* 78, 6381–6388.
37. Asokan, A., Conway, J.C., Phillips, J.L., Li, C., Hegge, J., Sinnott, R., Yadav, S., DiPrimio, N., Nam, H.J., Agbandje-McKenna, M., et al. (2010). Reengineering a receptor footprint of adeno-associated virus enables selective and systemic gene transfer to muscle. *Nat. Biotechnol.* 28, 79–82.
38. Dalkara, D., Byrne, L.C., Klimczak, R.R., Visel, M., Yin, L., Merigan, W.H., Flannery, J.G., and Schaffer, D.V. (2013). In vivo-directed evolution of a new adeno-associated virus for therapeutic outer retinal gene delivery from the vitreous. *Sci. Transl. Med.* 5, 189ra176.
39. Zinn, E., Pacouret, S., Khaychuk, V., Turunen, H.T., Carvalho, L.S., Andres-Mateos, E., Shah, S., Shelke, R., Maurer, A.C., Plovie, E., et al. (2015). In silico reconstruction of the viral evolutionary lineage yields a potent gene therapy vector. *Cell Rep.* 12, 1056–1068.
40. Niwa, H., Yamamura, K., and Miyazaki, J. (1991). Efficient selection for high-expression transfectants with a novel eukaryotic vector. *Gene* 108, 193–199.
41. Miyazaki, J., Takaki, S., Araki, K., Tashiro, F., Tominaga, A., Takatsu, K., and Yamamura, K. (1989). Expression vector system based on the chicken β-actin promoter directs efficient production of interleukin-5. *Gene* 79, 269–277.
42. Grieger, J.C., and Samulski, R.J. (2005). Packaging capacity of adeno-associated virus serotypes: impact of larger genomes on infectivity and postentry steps. *J. Virol.* 79, 9933–9944.
43. Choi, J.-H., Yu, N.-K., Baek, G.-C., Bakes, J., Seo, D., Nam, H.J., Baek, S.H., Lim, C.S., Lee, Y.S., and Kaang, B.K. (2014). Optimization of AAV expression cassettes to improve packaging capacity and transgene expression in neurons. *Mol. Brain* 7, 17.
44. Parmiani, G. (1998). Immunological approach to gene therapy of human cancer: improvements through the understanding of mechanism(s). *Gene Ther.* 5, 863–864.
45. Strobel, B., Miller, F.D., Rist, W., and Lamla, T. (2015). Comparative analysis of cesium chloride-and iodixanol-based purification of recombinant adeno-associated viral vectors for preclinical applications. *Hum. Gene Ther. Methods* 26, 147–157.
46. Harris, S.A., Enger, R.J., Riggs, B.L., and Spelsberg, T.C. (1995). Development and characterization of a conditionally immortalized human fetal osteoblastic cell line. *J. Bone Miner. Res.* 10, 178–186.

Supplemental Information

**Targeting Adeno-Associated Virus Vectors
for Local Delivery to Fractures
and Systemic Delivery to the Skeleton**

Lucinda R. Lee, Lauren Peacock, Leszek Lisowski, David G. Little, Craig F. Munns, and Aaron Schindeler

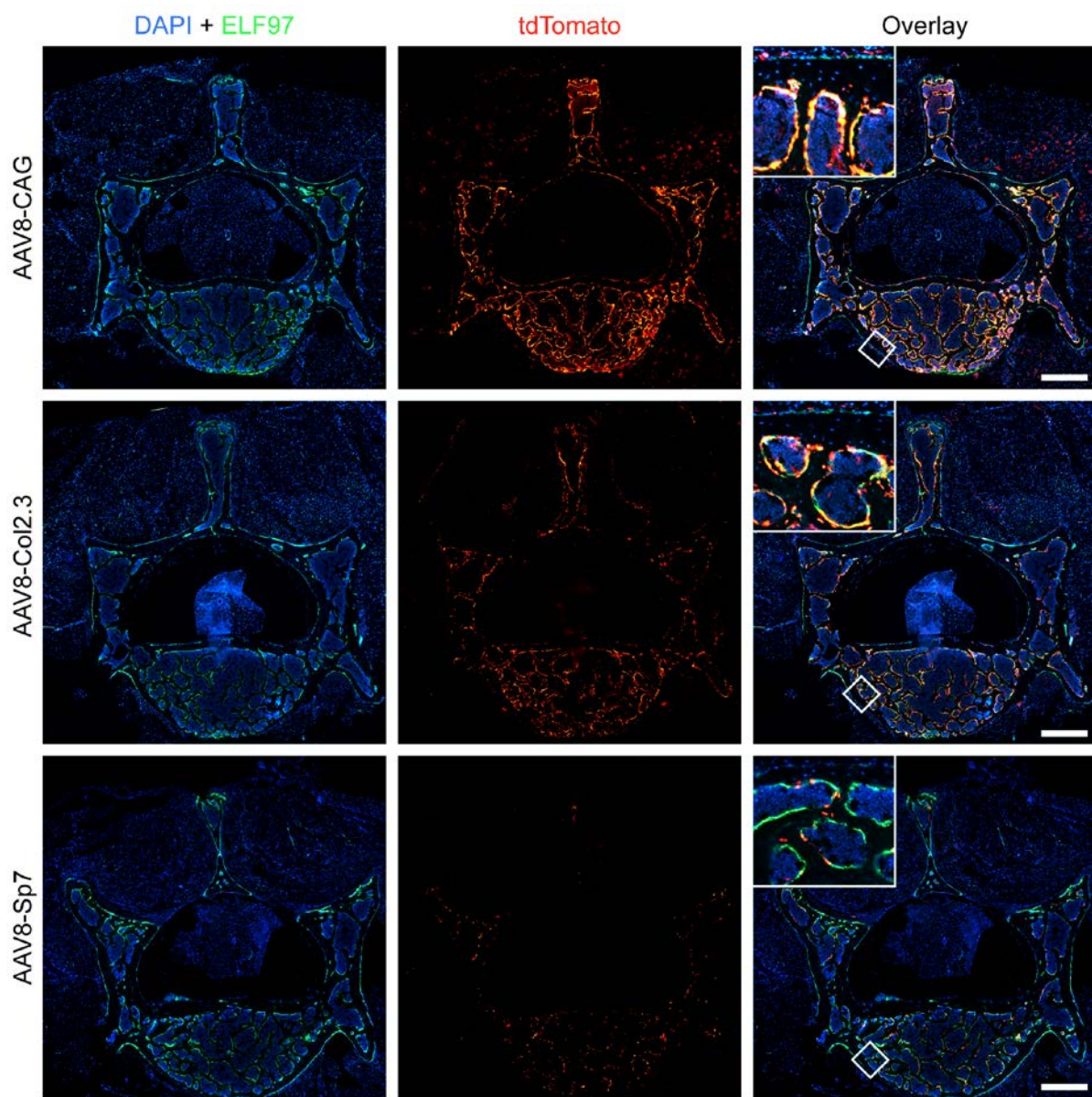
Supplementary Data

Supplementary Table 1: AAV variants tested in tibial fracture model with amount of viral genomes (vg) injected into each tibial fracture and visual grading of tdTomato expression within muscle, callus, and osteoblasts of tissue sections

Vector	Amount injected (vg)	tdTomato expression (muscle)	tdTomato expression (callus)	tdTomato expression (osteoblasts)
AAV1	2.46×10^{11}	+++	+	+
AAV2	9.50×10^{10}	+++	+++	++
AAV3	1.46×10^{11}	+++	+	+
AAV4	5.32×10^{11}	+	+	+
AAV5	2.18×10^{11}	+	+	-
AAV6	1.19×10^{10}	+	+	-
AAV8	5.94×10^{11}	+++	+++	+++
AAV9	3.24×10^{11}	+++	+++	+++
AAVrh10	1.87×10^{11}	+	+	+
AAV-DJ	1.81×10^{11}	+++	+++	+++
AAV-DJ8	2.48×10^{11}	+++	+++	++
AAV-2i8	9.40×10^{10}	+++	+	+
AAV-7m8	1.03×10^{11}	+	-	-
AAV-LK01	3.84×10^{10}	+	-	-
AAV-LK02	2.20×10^{11}	+	+	-
AAV-LK03	2.05×10^{11}	+++	+	-
AAV-LK19	1.89×10^{11}	+	-	-
AAV-Anc80	8.88×10^9	+++	+	+

	<i>AAV1</i>	<i>AAV2</i>	<i>AAV3</i>	<i>AAV4</i>	<i>AAV5</i>	<i>AAV6</i>	<i>AAV8</i>	<i>AAV9</i>	<i>AAVrh10</i>	<i>AAV-DJ</i>	<i>AAV-DJ8</i>	<i>AAV-2i8</i>	<i>AAV-7m8</i>	<i>AAV-LK01</i>	<i>AAV-LK02</i>	<i>AAV-LK03</i>	<i>AAV-LK19</i>	<i>AAV-Anc80</i>
MOI 1	8×10^5	3×10^5	5×10^5	9×10^5	7×10^5	8×10^4	1×10^6	6×10^5	5×10^5	6×10^5	4×10^5	3×10^5	3×10^5	1×10^5	4×10^5	3×10^5	6×10^4	
MOI 2	4×10^5	2×10^5	2×10^5	5×10^5	4×10^5	4×10^4	6×10^5	3×10^5	3×10^5	3×10^5	2×10^5	2×10^5	2×10^5	6×10^4	2×10^5	2×10^5	3×10^4	
MOI 3	2×10^5	6×10^4	1×10^5	4×10^5	1×10^5	2×10^4	4×10^5	1×10^5	2×10^5	1×10^5	2×10^5	6×10^4	7×10^4	3×10^4	1×10^5	1×10^5	1×10^5	
MOI 4	8×10^4	3×10^4	5×10^4	2×10^5	7×10^4	8×10^3	2×10^5	6×10^4	1×10^5	6×10^4	8×10^4	3×10^4	3×10^4	1×10^4	7×10^4	7×10^4	6×10^4	

Supplementary Figure 1: MOIs used for transduction of hFOB1.19 cells in Figure 4, expressed in vector genomes (vg) per cell



Supplementary Figure 2: Representative cryosections of L3 vertebrae from Ai9 mice receiving 5×10^{11} vg of AAV constructs, stained with ELF 97 for alkaline phosphatase.

Similar to the results for tibiae, high expression of tdTomato throughout the bone and muscle of the vertebral sections were detected in CAG samples. Col2.3 and Sp7 samples showed expression restricted to bone cells staining with ELF 97 and ELF 97 negative cells present within the bone matrix which appear to be osteocytes. Scale bars represent 500 μm .